identities hold quite well:

$$g[(h_{9/2}^2)J_p, j_n=\tfrac{1}{2}; I=J_p+\tfrac{1}{2}, {}^{209}\mathrm{Po}]$$
$$=[(2I-1)/2I]g(h_{9/2}, {}^{209}\mathrm{Bi})+(1/2I)g(p_{1/2}, {}^{207}\mathrm{Pb}),$$
$$B[E2, (h_{9/2}^2)J_p, j_n; I=J_p+j_n$$
$$\rightarrow(h_{9/2}^2)J_p', j_n; I'=J_p'+j_n]$$
$$=B[E2, (h_{9/2}^2)J_p\rightarrow(h_{9/2}^2)J_p'].$$

The level structure of ^{207}Po is rather different from that of ^{209}Po. In the ^{207}Po nucleus the ground state is the $f_{5/2}$ neutron hole state and the $i_{13/2}$ neutron hole state lies only at 1 MeV. The 47-μsec state may be the $i_{13/2}$ state. The highest spin of the $f_{5/2}$ hole coupled to the 8+ state of ^{210}Po is 21/2−, but the $E3$ character of the 2.5-sec 268-keV transition[8] limits the spin-parity of this long-lived isomeric state to 19/2, which is $2J_p+j_n-1$. This fact is consistent with the spin-parity 6+ of the ^{206}Bi ground state in which the $f_{7/2}^{-1}(n)$ and $h_{9/2}(p)$ orbits are coupled to $I=j_p+j_n-1$ in accordance with the Brennan-Bernstein rule.[29]

In ^{205}Po, only the $i_{13/2}$ isomeric state is established. The experiment is not conclusive as to the presence of another isomeric state involving the $(h_{9/2}^2)8+$ state of ^{210}Po.

[29] M. H. Brennan and A. H. Bernstein, Phys. Rev. **120**, 927 (1960).

G. Concluding Remarks

The present survey work has revealed a systematic presence of isomeric states in even and odd Po isotopes which involve the $(h_{9/2}^2)8+$ configuration. The present study has shown quite complex structures of isomerisms in these isotopes, and much should thus be done in the future, such as measurements of conversion electrons, decay measurements in expanded time scales and coincidence studies.

ACKNOWLEDGMENTS

The author would like to thank Dr. J. M. Hollander for his continuous encouragement and Dr. C. M. Lederer, Dr. S. G. Prussin, and Dr. J. M. Jaklevic for their help during this work. He is grateful to Dr. J. Blomqvist, Professor B. R. Mottelson, and Professor A. Arima for stimulating discussions. Finally, he expresses his gratitude to Professor I. Perlman and Professor J. O. Rasmussen for their hospitality at the Lawrence Radiation Laboratory.

PHYSICAL REVIEW C VOLUME 1, NUMBER 1 JANUARY 1970

Lifetimes and Nuclear Moments in Os^{192} and Pt^{192}

R. Béraud, I. Berkes, R. Chéry, R. Haroutunian, Michèle Lévy, G. Marguier, G. Marest, and R. Rougny
Institut de Physique Nucléaire, Université de Lyon-I, 69-Villeurbanne, France

(Received 24 July 1969)

Lifetimes, nuclear g factors, and $E2/M1$ mixing ratios have been determined in Os^{192} and Pt^{192}, and some previous determinations reevaluated. The following values have been established. For Os^{192}: $g_2=+0.29\pm0.05$; $\delta(484)=+7.6_{-1.3}^{+2.4}$. For Pt^{192}: $\tau_2=50.0\pm3.4$ psec; $\tau_2'=29\pm3$ psec; $g_2=+0.296\pm0.022$; $g_2'=+0.29\pm0.05$; $\delta(604)=+2.5\pm0.2$; $\delta(308)=-6.3_{-0.6}^{+0.5}$. Nuclear magnetic moments are analyzed in terms of Greiner's vibrational-rotational model, transition probabilities and $E2/M1$ mixing ratios are compared to the theoretical predictions of Kumar and Baranger's model.

I. INTRODUCTION

THE application of internal magnetic fields in iron alloys enables one to determine a great number of short-lived excited-state nuclear magnetic moments. Lifetime and nuclear moment data (until August 1967) are summarized in Ref. 1. The results on the first excited states in Pt nuclei show $g\simeq+0.3$; in Os^{192} the results on the first excited state are contradictory. Moreover, g factors of second excited 2^+ states are very scarce: for Dy^{160}, $g_{2'}=+0.18\pm0.06$[2]; for Os^{188}, $g_{2'}=+0.43\pm0.08$[3] or $+0.57\pm0.14$,[4] reevaluated with recent lifetime and internal field data by Shirley[1]; and for Pt^{194}, $g_{2'}=+0.15\pm0.04$.[5,6]

Our knowledge on lifetimes of second excited states in Pt nuclei is also very poor. The lifetime of Pt^{192}, determined by delayed coincidence of conversion electrons $\tau_{2'}=34\pm19$ psec,[7] has a large error; that of Pt^{194}, estab-

[1] *Hyperfine Structure and Nuclear Radiations*, edited by E. Matthais and D. A. Shirley (North-Holland Publishing Co., Amsterdam, 1968).
[2] R. Simon, I. Arens, R. S. Raghavan, and H. J. Körner, Phys. Letters **28B**, 590 (1968).
[3] J. Murray, T. A. McMath, and J. A. Cameron, Can. J. Phys. **45**, 1597 (1967).
[4] L. Keszthelyi, I. Demeter, I. Dézsi, and L. Pócs, Nucl. Phys. **A91**, 692, (1965).
[5] L. Keszthelyi, I. Berkes, I. Dézsi, and L. Pócs, Nucl. Phys. **71**, 662 (1965).
[6] Y. K. Agarwal, C. V. K. Baba, and S. K. Bhattacherjee, Nucl. Phys. **79**, 437 (1966).
[7] D. K. Butt and D. A. Jackson, Proc. Phys. Soc. (London) **86**, 31 (1965).

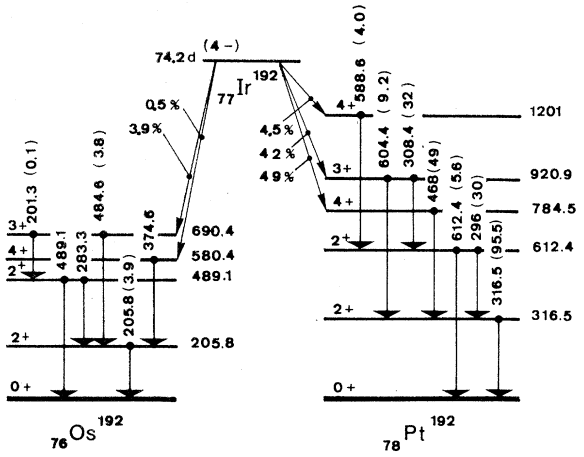

FIG. 1. Simplified decay scheme of the decay of Ir^{192}. Intensities (in brackets) are given for 100 desintegrations of Ir^{192}.

lished by Coulomb-excitation $\tau_{2'}=89\pm20$ psec, seems to be too high[8] as compared with that of Pt^{192} and also with theoretical estimations. The aim of this publication is to determine some missing or not well-known lifetimes and g factors in Os^{192} and Pt^{192}.

II. LIFETIME DETERMINATIONS

The simplified decay scheme of Ir^{192} is shown in Fig. 1.[9] To determine the lifetime of the 612-keV state, delayed coincidences between γ rays and K-conversion electrons were measured. The γ rays were detected by a 1×1-in. Naton 136 plastic scintillator mounted on a XP 1021 photomultiplier. In the slow channel, a discriminator selected, from the pulse-height spectrum of the detector, photons of $\simeq$600-keV energy. As this discriminator was set above the 468-keV γ line, it accepted the Compton edges of three γ rays: the 589-, 604-, and 612-keV γ rays, plus the Compton electrons of the weak 885-keV transition. Internal conversion electron groups were separated by a Gerholm-type lens spectrometer and detected also with a Naton 136+XP 1021 assembly. The energy spectrum of conversion electrons is shown on Fig. 2.

The time spectrum was analyzed with a fast time–to–pulse-height converter[10] and was displayed in coincidence with the lateral energy selection in a 100-channel subgroup of a 400-channel pulse-height analyzer. Time spectra taken at the top of the $e_K(316)$, $e_K(308)$, $e_K(296)$ electron peaks and at point C on the continuous β spectrum were registered in different subgroups. To avoid apparatus instability drifts, the temperature was stabilized and measurements were performed in 6-h runs. Since in the range considered the continuous β spectrum is nearly constant, the pure time distributions corresponding to the $e_K(296)$-$\gamma(600)$, $e_K(308)$-$\gamma(600)$, and $e_K(316)$-$\gamma(600)$ coincidences were obtained by subtracting the time spectrum taken at point C from the three other time spectra. To avoid delays due to the different transit times of conversion electrons versus energy through the spectrometer, the magnetic field was kept constant and the potential of the source was varied by an electrostatic accelerator-decelerator system. The only transit-time difference for the electrons arises during the acceleration on a path of a few centimeters and was taken into account.

As the discriminator on the slow γ channel is set on the Compton edge of the pulse-height distribution of the $\simeq$600-keV group, the mean energy of pulses accepted is proportional to the corresponding γ-ray energy. The $e_K(296)$-keV electron group is in coincidence with γ rays of 589-keV energy and the $e_K(308)$-keV electrons with $\gamma(612)$ keV. Thus, the difference in γ-ray energy gives rise to a first-order centroid shift. This electronic displacement has been determined in the same geometry and with the same detectors using a Co^{60} source, and the energy accepted in the γ channel was varied by changing the threshold of the single-channel pulse-height analyzer. Having applied these corrections, the centroid shift between the $e_K(296)$-$\gamma(600)$ and the $e_K(308)$-$\gamma(600)$ time distributions (see

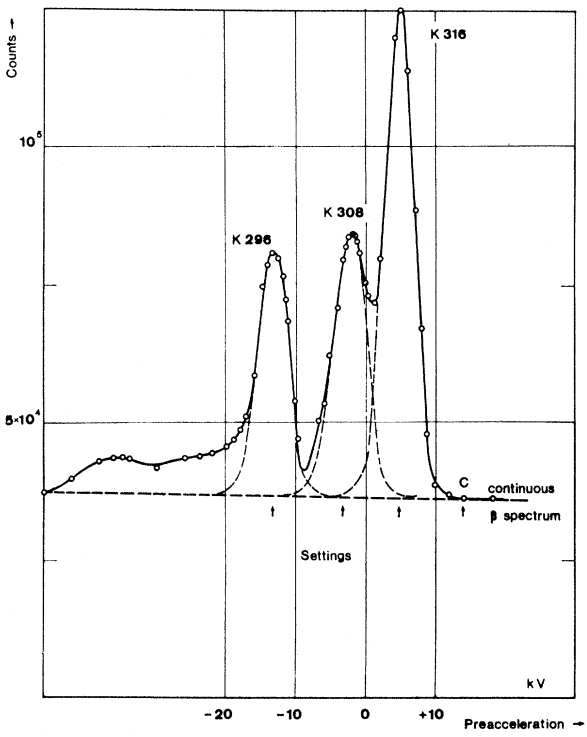

FIG. 2. Internal-conversion spectrum taken with the Gerholm-type lens spectrometer. The tail at the left side is composed from $L+M+N$ conversion peaks of the Os branch.

[8] F. K. McGowan and P. H. Stelson, Phys. Rev. **122**, 1274 (1961).
[9] C. M. Lederer, J. M. Hollander, and I. Perlman, *Table of Isotopes* (John Wiley & Sons, Inc., New York, 1967).
[10] J. J. Samuéli, J. Pigneret, and A. Sarazin, Nucl. Instr. Methods **28**, 330 (1964).

Fig. 3) gives $2\tau_{2'}=58\pm6$ psec, and thus

$$\tau_{2'}=29\pm3 \text{ psec.}$$

The $e_K(316)$-$\gamma(600)$ coincidences are composed from two distributions: the $\gamma(589)$-(296)-$e_K(316)$ triple correlation with unobserved intermediate radiation, with a delay of $\tau_2+\tau_{2'}$ with respect to the fictitious prompt distribution, and the $\gamma(604)$-$e_K(316)$ correlation with a time delay of τ_2. The contribution of the triple cascade is calculated as follows:

$$\text{coin}[\gamma(589)\text{-}(296)\text{-}e_K(316)]$$
$$=\text{coin}[\gamma(589)\text{-}e_K(296)]\alpha_K(316)/\alpha_K(296).$$

From the centroid shift between the $e_K(308)$-$\gamma(600)$ and $e_K(316)$-$\gamma(600)$ time-correlations, we obtain (by applying corrections mentioned above)

$$\tau_2=(89.7\pm5.0)-1.42\tau_{2'} \text{ psec,}$$

and with the second-excited-state lifetime determined above

$$\tau_2=48.5\pm6.5 \text{ psec.}$$

This value is in excellent agreement with that determined by Schwarzschild, using γ-γ delayed coincidences: $\tau_2=51\pm4$ psec.[11] Combining the two measurements gives

$$\tau_2=50.0\pm3.4 \text{ psec.}$$

In obtaining this mean value we did not take into account the $\tau_2=36\pm5$ psec value of de Boer,[12] published in 1962, because the deviation between this value and that accepted previously is about three times the standard deviation.

III. DETERMINATION OF g FACTORS AND TRANSITION MIXING RATIOS

A. Experimental

The short lifetimes of the excited states involved require the use of internal magnetic fields for the determination of nuclear g factors. For this reason the radioactive source was a dilute Ir-Fe alloy, containing 2% in weight of natural iridium, irradiated in a reactor. To let the Ir^{194} activity decay, measurements were started 2 weeks after irradiation. The source, forming a 2-mm-diam×5-mm cylinder was placed to bridge the gap of an electromagnet and magnetized to saturation for the perturbed angular-correlation measurements. The attenuation $G_k(\infty)$ defined by $W(\vartheta,\infty,B)=\sum G_kA_kP_k(\cos\vartheta)$ becomes for a nonmagnetized source, i.e., randomly oriented hyperfine fields.

$$G_k(\infty)=(2k+1)^{-1}+\sum_{m\neq m'}\begin{pmatrix} I & I & k \\ m & -m' & n\end{pmatrix}\frac{1}{1+(n\omega\tau)^2},$$

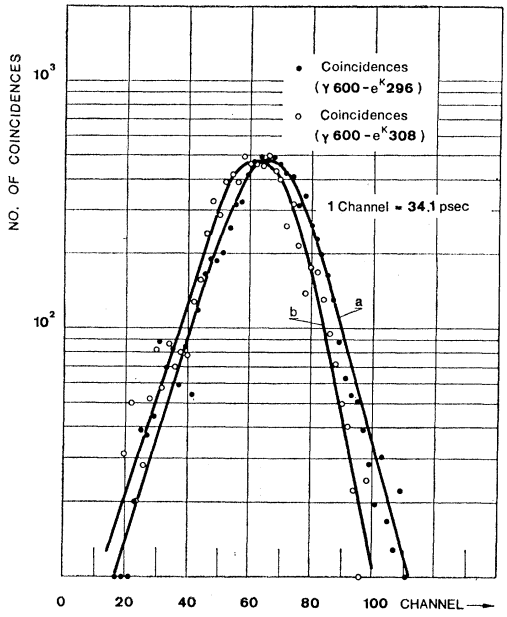

FIG. 3. Time correlation spectrum. Curve a: β channel setting on the 308-keV conversion line. Curve b: β channel setting on the 296-keV conversion line. Corrections discussed are included in the figure.

where ω is the Larmor precession angular velocity. For $I=2$, we have

$$G_k(\infty)=(2k+1)^{-1}\left(1+\sum_{n=1}^{k}\frac{2}{1+(n\omega\tau)^2}\right),$$

which was used to correct "nonperturbed" angular-correlation measurements.

Angular-correlation measurements were performed with a 30-cm^3 Ge(Li) detector in coincidence with a $1\frac{3}{4}$-in.-diam×4-in. NaI(Tl)+56 AVP scintillation counter. The coincidence spectrum of the Ge(Li) detector, taken with a fast-slow coincidence circuit, was displayed in the subgroups of a multichannel pulse-height analyzer. To evaluate angular correlations, the coincidence spectra of the Ge(Li) detector were decomposed numerically.

Four series of measurements were performed. In the first series, we determined the coefficients of the 468–316-, 604–316-, and 308–612-keV angular correlations in Pt^{192} and that of the 484–206-keV cascade in Os^{192}, with the nonmagnetized source. In a second series, the source was magnetized to saturation and perturbed angular correlations were measured for the same cascades as previously. To ameliorate statistics on the 308–612-keV correlation, in the third series, the 300–600-keV group coincidences have been registered twice, accepting in two different differential discriminator settings on the NaI(Tl) spectrum the 300- and 600-keV groups separately and stacking the Ge(Li) coincidence spectra in different memory blocks. In the fourth series, the asymmetry for field inversion has been measured at

[11] A. Schwarzschild, Phys. Rev. **141**, 1206 (1966).
[12] Th. J. de Boer *et al.*, Physica **28**, 417 (1962).

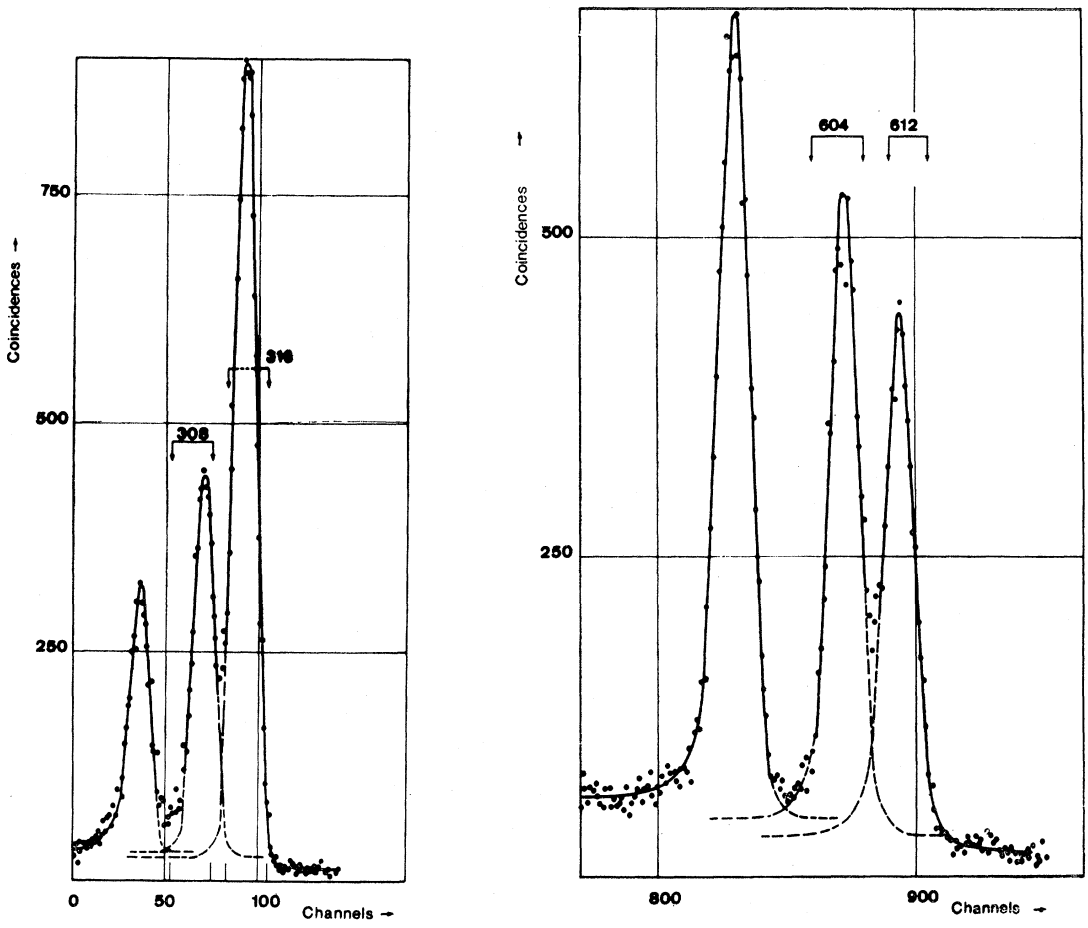

FIG. 4. Coincidence spectra of the Ge(Li) detector in the 300-keV (a) and 600-keV (b) range. Decomposition of the peaks and the range of numerical integration for each peak are shown on the figure.

angles near the maximum asymmetry, and the rotation of the angular correlation was evaluated using previously determined angular-correlation coefficients.

The organigram of the measurements appears in Table I.

To avoid systematic errors due to eventual gain drift, the temperature was stabilized and the magnetic field direction inverted every 500 sec.

B. Data Treatment and Results

The coincidence spectra for the Ge(Li) detector, taken at 210° in the 300- and 600-keV ranges, are shown on Fig. 4. For the evaluation of angular correlation, coincidence intensities were obtained by numerical integration of the corresponding photopeaks. Doing this, some precautions have to be taken.

1. 468 316-keV Cascade

This cascade was measured in two different ways (see Table I). When the Ge(Li) detector accepts the 468-keV radiation, the angular correlation measured is free from systematic errors. When the Ge(Li) detector accepts the 316-keV line, the angular correlation contains a small proportion of 589-(296)-316- and 604-316-keV correlations, due to the Compton spectra of the 589- and 604-keV γ rays in the NaI(Tl) detector. Having corrected for these effects, by using the intensity of the 296-keV peak (Ge-Li) in coincidence with the 468-keV band (NaI), the result agrees with that obtained formerly. The angular correlation coefficients, corrected for rotation and finite solid-angle attenuation agree with the theoretical 4-2-0 coefficients (Fig. 5).

2. 604–316-keV Cascade

If the 316-keV peak is taken in the Ge(Li) detector, the angular correlation contains the 589-(296)-316-keV cascade too. Corrected for, as previously, the angular-correlation coefficients agree with the 604(Ge-Li)-316(NaI) determination.

The corrections, mentioned above, affecting the

TABLE I. Organigram of angular-correlation measurements. The *italicized* energies are those whose corresponding photopeak can be evaluated from the Ge(Li) coincidence spectrum.

Angles	Magnetic field	Determined	Series No	Registered energy range for Ge(Li) detector in coin. with NaI (keV)	Selected NaI(Tl) energy range (keV)	Angular correlation	Remark
9 angles from 90° to 270°	no	Angular-correlation coefficients by computer fitting	1	200–650	468+484	468–*316*	Pt^{192}
						484–*206*	Os^{192}
					589+604+612	589–*296*	
						308–612	Pt^{192}
						589–(296)–*316*+ 604–*316*	
	$\pm B$	Angular-correlation coefficients and rotation of angular-correlation pattern by computer fitting	2		as previously		589–*296* not evaluated
			3	280–650	296+308+316	*589*–296+ *589*–(296)–316	not evaluated
						308–*612*	
						604–316	Pt^{192}
						468–316	
					589+604+612	589–*296*	not evaluated
						612–*308*	
						589–(269)–*316* +604–*316*	Pt^{192}
150° and 210°	$\pm B$	Asymmetry for $\pm B$	4		as previously		

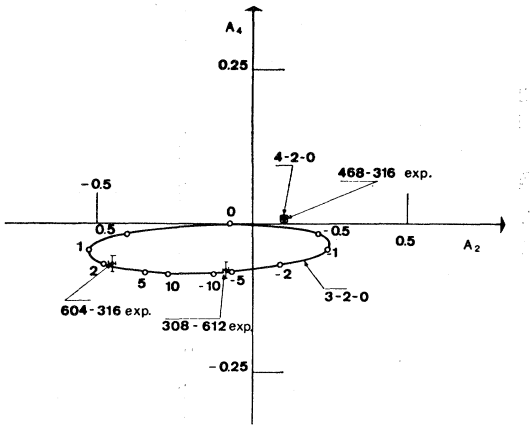

FIG. 5. Graphical analysis of angular-correlation measurements on the $[A_2A_4]$ plot. Some $\delta=E2/M1$ mixing parameters are indicated on the plot. The phase sign convention is identical to that in Table II.

angular-correlation coefficients do not influence in any case the precision of the rotation of the angular-correlation pattern, which must be corrected only if nonisotropic angular correlations with different intermediate states are superposed (cf. Sec. III C 1).

3. 308–612-keV Cascade

On account of the great anisotropy of the 604–316-keV angular correlation, the precise subtraction of the contribution of the 316-keV peak to the 308-keV photopeak is very important. The decomposition was determined using the pulse-height distribution of the 321-keV line of a Cr^{51} source (see Fig. 4).

The over-all results of the four series of measurements are summarized in Table II.[13,14]

C. Comparison of Experimental Results

1. Mixing Parameters of the 308- and 604-keV Radiations

On Fig. 5, we show on an A_2-A_4 plot our angular-correlation coefficients and compare them with theoretical 4-2-0 and 3-2-0 correlations. On this plot, every (A_2, A_4) point lies, within the experimental accuracy, on the ellipse corresponding to the supposed spin sequence. While our 604–316-keV angular-correlation coefficients are in rather good agreement with those of Refs. 15 and 16, the coefficients of the 308–612-keV angular correlations are different in each measurement (cf. Tables II and III). The A_4 coefficient for a 3-2-0 cascade in this region of A_2 should be about $A_4=-0.081$ for $\delta^2\gg1$ or $0\geq A_4\geq-0.01$ for $\delta^2\ll1$. The A_4 values of Refs. 15 and 16 do not allow one to obtain the quoted mixing ratios.

TABLE II. Results of angular-correlation measurements. The phase sign of δ is that of Rose and Brink (Ref. 14). Theoretical mixing ratios are from the work of Kumar (Ref. 13).

Nucleus	Intermediate state	Spin sequence	Angular correlation A_2	Angular correlation A_4	Rotation of the intermediate state (mrad)	$\delta(E2/M1)$ mixing ratio Transition	Expt	Theor
Os^{192}	206	3-2-0	-0.304 ± 0.021	-0.06 ± 0.05	600 ± 85	484	$+7.6_{-1.3}^{+2.4}$	+4.8
Pt^{192}	316	4-2-0	$+0.104\pm0.002$	$+0.009\pm0.003$	82.5 ± 5.8	...	...	...
Pt^{192}	316	3-2-0	-0.450 ± 0.010	-0.065 ± 0.013	88.4 ± 2.6	604	$+2.5\pm0.2$	+2.2
Pt^{192}	612	3-2-0	-0.084 ± 0.010	-0.075 ± 0.012	53 ± 9	308	$-6.3_{-0.6}^{+0.5}$	−9.2

[13] K. Kumar, Phys. Letters **29B**, 25 (1965).
[14] H. J. Rose and D. M. Brink, Rev. Mod. Phys. **39**, 306 (1967).
[15] W. D. Hamilton and K. E. Davies, Nucl. Phys. **A122**, 165 (1968).
[16] D. B. Kenyon, L. Keszthelyi, and J. A. Cameron, Can. J. Phys. **47**, 2395 (1969).

TABLE III. Comparison of recent $E2/M1$ mixing-parameter determinations from (308–612)-keV angular-correlation measurements in Pt^{192}. Phase convention of δ is that of Rose and Brink (Ref. 14). [The $A_4=-0.023\pm0.020$ value in the paper of Hamilton and Davies (Ref. 15) has been corrected by the authors to give -0.043 ± 0.020].

A_2	A_4	δ deduced	Authors	Ref.
-0.094 ± 0.015	-0.043 ± 0.020	-6.5 to -8.3	Hamilton-Davies	15
-0.120 ± 0.020	-0.027 ± 0.020	-9.4 ± 1.5	Kenyon *et al.*	16

By angular-distribution measurements on oriented nuclei, Reid, Šott, and Stone determined recently the mixing parameters of the 308- and 604-keV radiations.[17] For the 308-keV transition, their value $\delta=-7.3\pm0.2$ (using our phase convention) is only slightly higher than ours, in absolute value. For the 604-keV transition, they find $\delta=+1.5\pm0.10$. This value would yield in the 604–316-keV angular correlation $A_2=-0.52$, which is too high compared to our value, and also to the previously obtained values $A_2=-0.480\pm0.016$ [15] and $A_2=-0.410\pm0.015$.[16] On the other hand, a mixing parameter $\delta>+2$, derived from the angular correlation experiments, would impose an intermediate-state depolarization factor greater than 1 to fit the orientation distribution. As the nuclear orientation distribution is very sensitive to δ in this range, the disagreement between orientation and angular-correlation experiments seems to be outside of the experimental accuracy.

2. $\omega\tau$ of the First Excited State in Os^{192}

The Larmor precession of excited-state nuclear moments in the Ir-Fe alloy has been already investigated for the Os^{192} and Pt^{192} first excited states, and simultaneously with us also for the second excited state of Pt^{192}. We summarize these values in Table IV.

The results on the g factor of Os^{192} first excited state are in striking disagreement with each other. In the first measurement of Table IV, the differential discriminator accepted the (468+484)-keV composed photopeak in a NaI(Tl) detector, and in the second NaI(Tl) detector the 206-keV photopeak must be decomposed from the Compton distribution of the 316-keV ray. To reduce decomposition problems, Pramila selected a small band on the upper end of the (468+484)-keV photopeak.[18] Her rotation and attenuation measurements are, however, in disagreement and she accepted the rotation value. The great straggling in $\omega\tau$ values is certainly due to the decomposition of the NaI(Tl) pulse-height spectrum.

3. $\omega\tau$ of the First Excited State in Pt^{192}

To determine the g factor of the first excited state of Pt^{192}, we used in this measurement two angular correlations: the 468–316-keV (4-2-0) cascade and the 604–316-keV (3-2-0) cascade. The two results being in agreement, they may be combined to give $\omega\tau=87.5\pm2.4$

TABLE IV. Larmor precession angles in dilute Ir-Fe alloys.

Nucleus	State	$\omega\tau$ mrad	Detector	Reference	Remark
Os^{192}	2^+	235 ± 34	NaI-NaI	4	Coincidence spectrum
		410 ± 60	NaI-NaI	18	Rotation measurement
		$\simeq600$	NaI-NaI	18	Attenuation of angular correlation
		600 ± 85	Ge(Li)-NaI	This work	
Pt^{192}	2^+	68 ± 7	NaI-NaI	21	
		92 ± 8	NaI-NaI	19	
		63 ± 9	NaI-NaI	5	600–600-keV cascade and 468–300-keV cascade
		80 ± 5	NaI-NaI	6	Mean value of three different alloys
		88 ± 5	Ge(Li)-NaI	16	
		87.5 ± 2.4	Ge(Li)-NaI	This work	
Pt^{192}	2^+	47 ± 11	Ge(Li)-NaI	16	
		53 ± 9	Ge(Li)-NaI	This work	

[17] P. G. E. Reid, M. Šott, and N. J. Stone, Nucl. Phys. A129, 273 (1969).
[18] G. C. Pramila, Ph.D. thesis, MIT, 1967 (unpublished).

TABLE V. Comparison between experimental and theoretical nuclear g factors in Os^{192} and $Pt^{192-198}$ nuclei. Where more than one reference is given, we took the weighted mean value. Magnetic field values are those of Kontani and Itoh (Ref. 22), corrected for room temperature, except that for Pt^{198} where it is the dynamical value after Coulomb implantation given by Kalish *et al.* (Ref. 26).

Nucleus	State	Rotation angle (mrad)	Ref. rotation	Magnetic field T	Lifetime psec	Ref. lifetime	g Expt	g Calc
Os^{192}	206	600±85	This work	−111±2	393±40	23	+0.29±0.05	0.311
Pt^{192}	316	87.5±2.4	This work	−123.5±2.0	50.0±3.4	This work	+0.296±0.022	0.325
	612	50.5±7.0	This work	−123.5±2.0	29±3	This work	+0.29±0.05	0.323
Pt^{194}	329	96.0±3.2	24	−123.5±2.0	51±5	23	+0.319±0.035	0.320
	622	80±12	5, 6	−123.5±2.0	89±20	1	+0.15±0.03	0.319
Pt^{196}	356	83.4±3.5	24, 25	−123.5±2.0	47±5	24	+0.286±0.035	0.315
Pt^{198}	408	30.5±0.2	26	−89±7	25.5±3.0	26	+0.28±0.04	0.314

mrad. This value is in excellent agreement with the recent value of the McMaster group[16] and with the MIT result.[19] The lower value of the Tata group[6] is probably due to the fact that they used three sources: a dilute alloy with 3.3 wt % Ir in Fe, an alloy of 7.2 wt % Ir, and a diffused source. The field-up–field down asymmetry at 45° was successively: (1.65±0.10), (1.50±0.11), and (1.49±0.10)%. As the diffused and the 7.2% Ir source gave the same value, the authors concluded that the deviation from the dilute alloy rotation should be only of a statistical nature and composed their mean value. It is possible, however, that the diffusion was not perfect and the averaged hyperfine field acting on the nucleus was diminished. Such an effect has already been reported by the MIT group.[20] If this were the case, the Tata result should be rather $\omega\tau=$ 88±8 mrad.

Two values deviate considerably from ours: the older McMaster result[21] and the Budapest value.[5] In using the 468–316-keV angular correlation, the 468-keV channel may accept, depending on the setting, a small proportion of the very anisotropic 604–316-keV angular correlation; if the rotation $\omega\tau$ is determined by measuring the asymmetry at one angle, by reversing the magnetic field direction, the setting of the 468-keV channel must be completely identical to that used for the measurement of the angular-correlation coefficient. If this is the reason for the low value of $\omega\tau$ in Ref. 21, the Budapest result is not affected by this error. These authors determined the rotation by using both the 468–316- and 600–300-keV groups and obtained: $\omega\tau=69\pm20$ and 61±10 mrad, respectively. This latter angular correlation contains, besides the 604–316-keV cascade, the 589–296- and the 589–(296)–316-keV nearly isotropic angular correlations, the 589–612 keV cascade twice (rotating in opposite directions), and the 308–612-keV cascade, going through the 612-keV level and rotating in the opposite direction to the 604–316-keV correlation with $\omega\tau=50$ mrad. Letting b_2' and b_2'' be the angular-correlation coefficients of two superposed cascades (we neglect the $\cos4\vartheta$ contribution), α' and α'' the corresponding rotation angles, a the contribution of the first cascade in the measurement, and $\langle\alpha\rangle_{av}$ the mean rotation angle in the superposed correlations, we find for $\omega\tau=\alpha\ll1$

$$\langle\alpha\rangle_{av}=\frac{ab_2'\alpha'+(1-a)b_2''\alpha''}{ab_2'+(1-a)b_2''}.$$

With the known intensity ratios[9] and angular-correlation coefficients, we find that the Budapest measurement should give for the 604–316-keV angular correlation $\alpha'=72$ mrad and the composed mean value of this and the 468–316-keV measurement becomes 71±9 mrad, somewhat nearer to the more recent values.

4. $\omega\tau$ of the Second Excited State in Pt^{192}

The recent measurement of the McMaster group gives for the second excited state of Pt^{192} $\omega\tau=47\pm11$ mrad. This value is in excellent agreement with our result (Table IV); the mean value of the two measure-

TABLE VI. Electromagnetic transition probabilities in Pt^{192}. Calculated values are taken from Ref. 28.

Transition	Energy (keV)	$10^{48}B(E2)$ (e^2 cm^4) Expt	Calc	$10^{+3}B(M1)$ (nm^2) Expt	Calc
2→0	316	0.48±0.04	0.362		
2′→0	612	0.0050±0.0005	0.0010		
2′→2	296	0.93±0.09	0.555	0.2–1.2	0.155
4→2	468	0.21±0.04	0.556		

[19] A. Buyrn and L. Grodzins, MIT Report No. 2098-142, 1964 (unpublished).
[20] A. Buyrn and L. Grodzins, MIT Report No. 2098-251, 1965 (unpublished).
[21] J. A. Cameron, Can. J. Phys. 42, 1680 (1964).

TABLE VII. Comparison of electromagnetic properties of the second excited states in platinium nuclei.

Nucleus	$R_1=B(E2;2'\rightarrow2)/B(E2;2\rightarrow0)$ Expt	Calc[a]	$R_2=g_{2'}/g_2$ Expt	Calc	R_1/R_2 Measured
Pt^{192}	1.94±0.25	1.54	0.99±0.19	1.0	1.96±0.27
Pt^{194}	0.87±0.22	1.32	0.47±0.15	1.0	1.85±0.27

[a] Reference 28.

ments is $\omega\tau=50.5\pm7.0$ mrad. This value will be used for the g-factor evaluation.

5. *Nuclear g Factors*

To determine the nuclear g factors, we used the magnetic hyperfine fields, determined by Kontani and Itoh,[22] corrected by $\simeq2\%$ for room temperature. Nuclear g factors are summarized in Table V.[23–26] The measurements yield directly $g_2'/g_2=0.99\pm0.19$.

An external field g-factor determination has been performed by Coulomb excitation on Os^{192} by Gilad *et al.*[27] The g factor, reevaluated for the lifetime value of Table V would be $g_2=+0.41\pm0.05$. This value seems to disagree with theoretical estimations.

IV. DISCUSSION

The lifetime values established in Sec. II allow the determination of some transition probabilities in Pt^{192} which we summarized in Table VI.[28] The two $B(M1;2'\rightarrow2)$ values given correspond to $\delta=15$ [17] and $\delta=6.7$.[29] On account of the uncertainty in δ being larger than experimental errors quoted, these $B(M1)$ values are merely suggestive. The $B(E2;4\rightarrow2)$ value is derived from the lifetime of the 785-keV level determined by Schwarzschild.[11] Branching ratios and internal-conversion coefficients used were taken from Ref. 9.

In the same Table, we compare the experimental transition probabilities with the theoretical values of Kumar and Baranger based on the pairing-plus-quadrupole model. The agreement for the stop-over transitions is rather good, but the crossover transition seems to be less forbidden than in the theoretical model.

Unfortunately, their g factors in Pt nuclei are lower by about 35% than experimental values. It has to be mentioned that the inclusion of the dynamics into the calculations gives a worse agreement between theoretical and experimental g factors.[23]

As the magnetic dipole moment is a state parameter, one may try to understand it in a phenomenological way. Sakai has classified the levels of Os and Pt nuclei in pseudo-ground-state and pseudo-γ-bands.[30] In this way we calculated the Os and Pt g factors with Greiner's model[31] mixing mainly the $K=0$ ground state and $K=2$ γ bands. The values of E_β, E_γ, and β_0 were taken from Ref. 32. Calculated g factors are compared with experimental ones in Table V. All measured g factors, except that of the second excited state of Pt^{194} (to be discussed below), agree within the experimental errors with the calculations. There is, however, a general tendency to have our calculated g factors slightly above experimental ones. While g factors of Pt^{192} calculated from different models differ, that of the Os^{192} first excited state is almost identical in all predictions,[28,32,33] and agrees well with our experimental value.

An important feature of all the models discussed is that the g factors of the first and second excited 2^+ states are nearly the same, the greatest deviation being about 10%. While this prediction is confirmed for the Pt^{192}, the g_2' in Pt^{194} is about half of g_2. In Table VII, we compare the characteristics of the second 2^+ states in Pt^{192} and Pt^{194}. While not only calculated g_2'/g_2 are identical, but also theoretical $B(E2;2'\rightarrow2)/B(E2;2\rightarrow0)$ ratios are very near in the two isotopes, the experimental ratios vary by more than a factor of 2. The experimental ratio R_1/R_2 (Table VII), derived directly from the rotation angles, being thus independent from the experimental determination of τ_2', is also the same for the Pt^{192} and Pt^{194} nuclei. As it seems that the difficulties in the interpretation of Pt^{194} results are due to the lifetime value of the second excited state, its redetermination, either by a direct lifetime measurement, or by Coulomb excitation, using recent experimental techniques, would be of great interest.

ACKNOWLEDGMENTS

The authors are indebted to Professor K. Kumar, Professor J-N. Massot, and Dr. I. A. Campbell for helpful discussions, to Dr. J. A. Cameron and Dr. L. Keszthelyi for communicating their results prior to publication, and to Dr. R. Lemaire for the alloy preparation.

[22] M. Kontani and J. Itoh, J. Phys. Soc. Japan 22, 345 (1967).
[23] P. H. Stelson and L. Grodzins, in *Nuclear Data Tables* (Academic Press Inc., New York, 1965), Sec. A, Vol. 1, No. 1.
[24] R. Béraud, I. Berkes, J. Danière, Michèle Lévy, G. Marest, and R. Rougny, Ref. 1, p. 199.
[25] J. Murray, T. A. McMath, and J. A. Cameron, Can. J. Phys. 46, 75 (1968).
[26] R. Kalish, L. Grodzins, R. R. Borchers, J. D. Bronson, and B. Herskind, Phys. Rev. 161, 1196 (1967).
[27] P. Gilad, G. Goldring, R. Herber, and R. Kalish, Nucl. Phys. A91, 85 (1967).
[28] K. Kumar and M. Baranger, Nucl. Phys. A122, 273 (1968).
[29] J. Koch, F. Münnich, and U. Schötzig, Nucl. Phys. A103, 300 (1967).
[30] K. Kumar and M. Baranger, Nucl. Phys. A110, 529 (1968).
[31] M. Sakai, Nucl. Phys. A104, 301 (1967).
[32] W. Greiner, Nucl. Phys. 80, 417 (1966).
[33] O. Prior, F. Boehm, and S. G. Nilsson, Nucl. Phys. A110, 257 (1968).